S. Afr. J. Chem., 2007, **60**, 76–84,
<http://journals.sabinet.co.za/sajchem/>.

Binary Molecular Complexes and the Nature of Molecular Association†

T. Anthony Ford*

Centre for Theoretical and Computational Chemistry, School of Chemistry, University of KwaZulu-Natal, Westville Campus, Private Bag X54001, Durban, 4000 South Africa.

Received 14 May 2007, revised 23 August 2007, accepted 24 August 2007.

ABSTRACT

A survey is presented of the results of some *ab initio* calculations of the properties of a variety of binary molecular complexes. The properties include the molecular structures, the interaction energies and the vibrational spectra. The interaction energies have been correlated with some physical properties of the interacting monomer species, and the changes in the values of the monomer structural parameters, and the vibrational wavenumber shifts occurring on complexation have been correlated with the interaction energies. The range of molecular complexes studied covers examples from the hydrogen-bonded, blue-shifting hydrogen-bonded, halogen-bonded and electron donor-acceptor types. Some generalizations concerning the nature of molecular association have been presented.

KEYWORDS

***Ab initio* calculations, molecular complexes, molecular structures, interaction energies, vibrational spectra.**

1. Introduction

Research in this laboratory has focused for several years on the nature of the various types of molecular association commonly encountered in binary molecular complexes. In our investigations we have studied a variety of hydrogen-bonded,[1–4] electron donor-acceptor (EDA)[5–8] and van der Waals complexes,[9–12] in an attempt to elucidate the features common to the various families of molecular interactions, and the essential differences which distinguish one type of association from another. The ultimate aim of this research was to formulate a unified theory covering the whole spectrum of molecular associations. Such a theory should be sufficiently robust to allow predictions of the properties of complexes formed between any pair of interacting monomers and to compare the values of those properties with those of related families of complexes, thus identifying the fundamental properties of the monomers which chiefly govern the natures of the resulting complexes. In this publication we survey some recent *ab initio* theoretical results related to examples of complexes drawn from two of the families of molecular interaction referred to above, hydrogen-bonded and EDA, and describe some investigations of aggregates which exhibit two newer types of interaction, blue-shifting hydrogen bonding and halogen bonding. Some similarities among the various families of complexes are pointed out.

2. Computational Details

The calculations were all carried out using the Gaussian-98 computer program package[13] at the second order level of Møller-Plesset perturbation theory.[14] We employed a triple-zeta split valence Gaussian basis set, with polarization and diffuse functions on all atoms, designated 6-311++G(d,p).[15,16] Geometry optimizations were carried out on all monomer and complex molecules, using the VERYTIGHT convergence criterion,[13] to ensure proper convergence to the true energy minimum of each species. Identification of genuine potential energy minima, and distinction between true minima and transition states, was accomplished by carrying out vibrational analyses, using analytical gradients. Interaction energies were determined by simple subtraction, and were corrected for basis set superposition error (BSSE)[17] by the full counterpoise method of Boys and Bernardi,[18] and for vibrational zero-point energy differences.

3. Results and Discussion

3.1. Hydrogen-bonded Complexes

The hydrogen bond was first named by Latimer and Rodebush[19] in 1920. The essential features are an acid containing an AH group, where A is usually N, O, F, P, S or Cl, in which the hydrogen atom is slightly positively charged, as the proton donor (electron acceptor), and a base containing an atom B, where B is commonly N, O, P or S, as the proton acceptor (electron donor). The physical manifestations of the presence of a hydrogen bond are an increase in the AH bond length, a shift of the AH stretching wavenumber to the red and an enhancement of the infrared intensity of the AH stretching band, relative to their values in the non-interacting monomer.[20] We have selected as examples of hydrogen-bonded complexes for study those formed between methanol as proton donor and trimethylamine, dimethyl ether, methyl fluoride, trimethyl phosphine, dimethyl sulphide and methyl chloride as proton acceptors. In this way we compare the properties of the OH…N, OH…O, OH…F, OH…P, OH…S and OH…Cl types of complexes and determine how these properties change as the electron donor atom changes from group 15 to group 17 and from the first to the second row of the periodic table. Steric and electronic influences are eliminated by choosing as bases only those with methyl groups attached to the proton acceptor atom. Thus the only determinants of the properties of the complexes are associated with the nature of the electron donor atom. The optimized structures of these six complexes are illustrated in Fig. 1. The

†The SACI Gold Medal Lecture 2006. This paper was presented at the 38th South African Chemical Institute Convention, Durban, 3–8 December 2006.

*E-mail: ford@ukzn.ac.za

Table 1 Interaction energies of some hydrogen-bonded complexes.

First row bases		Second row bases	
System	ΔE/kJ mol^{-1}	System	ΔE/kJ mol^{-1}
OH…N	–25.1	OH…P	–13.4
OH…O	–16.2	OH…S	–12.2
OH…F	–10.2	OH…Cl	–8.0

computed interaction energies are presented in Table 1. The strength of interaction decreases regularly in the series N > O > F and P > S > Cl, and the complexes with the first row bases are consistently more strongly bound than those from the second row. The interaction energies correlate well with the gas phase basicities[21] of the electron donors, as shown in Fig. 2, with separate relationships for the first and second row bases.

The structural properties (OH bond lengths and their changes, O…B separations, H…B separations and OH…B bond angles) are shown in Table 2. The perturbations of the OH bond lengths parallel the strengths of interaction, but the O…B and H…B distances do not seem to exhibit any pattern. The OH…B angles are quite close to the optimum value of 180° for the N, O and P bases, but for OH…S, OH…F and OH…Cl the angles indicate quite substantial deviation from linearity. Inspection of Fig. 1 shows that in the OH…S case, there is a secondary site of interaction, between two of the methyl hydrogen atoms of $(CH_3)_2S$ and the oxygen atom of CH_3OH. This secondary interaction can be accommodated by a bending of the OH…S angle away from linearity. Similar secondary interactions are found in the OH…F and OH…Cl aggregates. In these cases the hydrogen atoms of CH_3F and CH_3Cl lying in the symmetry plane of the complex are attracted to the oxygen atom of CH_3OH, resulting in the formation of a five-membered ring containing a weak CH…O interaction. The increases of the OH bond lengths are dependent

Table 2 Structural properties of the various OH…B hydrogen-bonded systems.

System	r(OH) /pm	Δr(OH) /pm	R(O…B) /pm	R(H…B) /pm	∠OH…B /deg
OH…N	97.87	1.93	282.72	184.87	178.50
OH…O	96.77	0.83	281.73	185.00	178.18
OH…F	96.17	0.23	287.97	204.12	144.61
OH…P	96.73	0.79	345.20	248.53	177.62
OH…S	96.63	0.69	326.17	240.44	147.61
OH…Cl	96.13	0.19	329.98	256.05	133.82

Table 3 Spectroscopic properties of the various OH…B hydrogen-bonded systems.

System	$\bar{\nu}$(OH)/cm^{-1}	Δ$\bar{\nu}$OH)/cm^{-1}	A(complex) /km mol^{-1}	A(complex) /A(monomer)
OH…N	3505.0	–408.6	1060.2	29.4
OH…O	3748.8	–164.8	580.2	16.1
OH…F	3879.8	–33.8	143.9	4.0
OH…P	3748.3	–165.3	565.9	15.7
OH…S	3768.1	–145.5	329.7	9.2
OH…Cl	3883.8	–29.8	103.1	2.9

on the interaction energies, where again separate relationships are observed for the first and second row bases. The spectroscopic properties of the complexes (the OH stretching wavenumbers and their shifts, and the OH stretching infrared intensities and their ratios to that of the methanol monomer) are collected in Table 3. The magnitudes of the shifts, and the enhancements of the intensities, are directly related to the interaction energies, typical of many other hydrogen-bonded systems.

The orbital interactions involved in the formation of a conven-

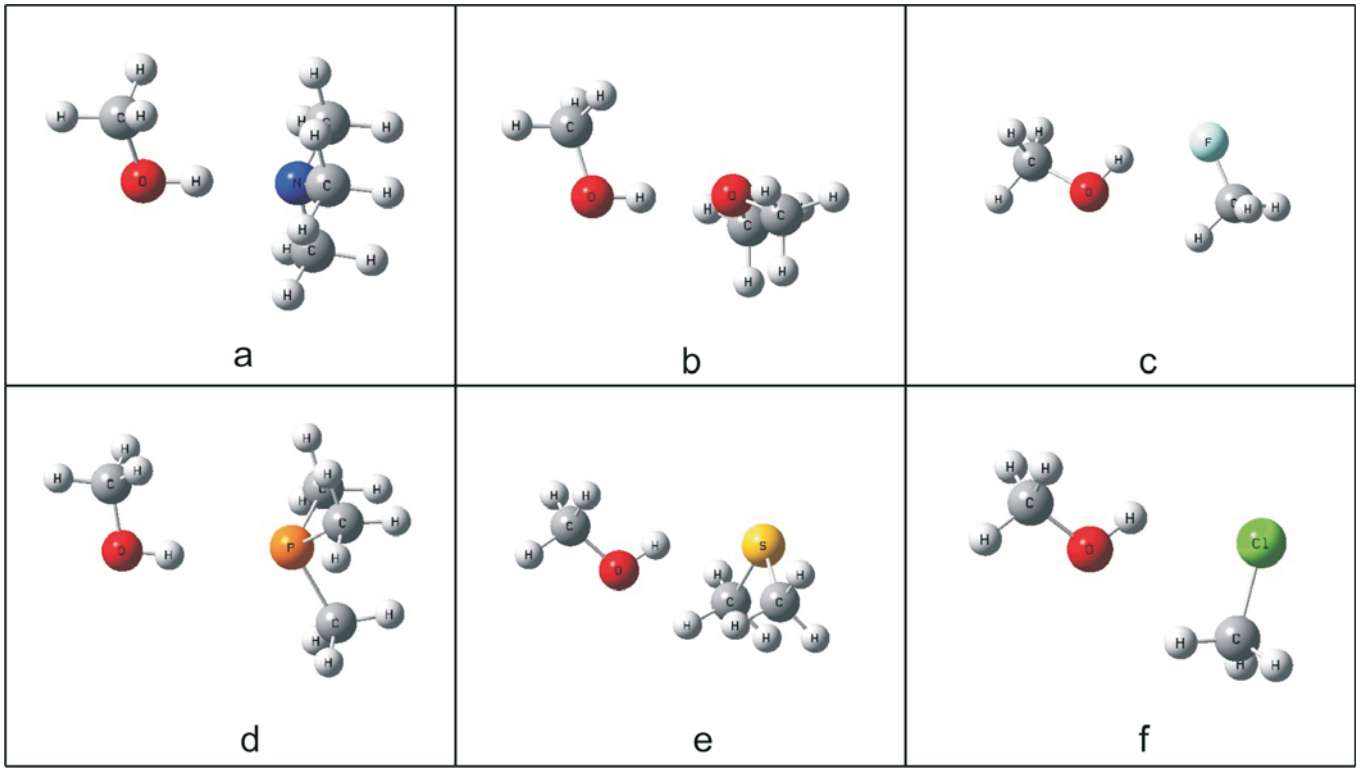

Figure 1 The optimized structures of the hydrogen-bonded complexes of CH_3OH with (**a**) $(CH_3)_3N$, (**b**) $(CH_3)_2O$, (**c**) CH_3F, (**d**) $(CH_3)_3P$, (**e**) $(CH_3)_2S$ and (**f**) CH_3Cl.

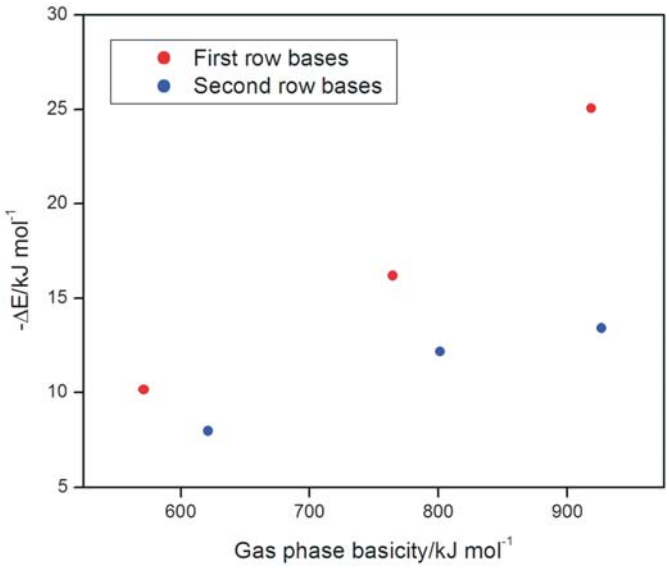

Figure 2 Plots of the interaction energies of some complexes of CH_3OH *versus* the gas phase basicities of the proton acceptors.

tional hydrogen bond are exemplified by considering the LUMO (8a′) of CH_3OH (OH σ antibonding) and the HOMO ($6a_1$) of $(CH_3)_3N$ (non-bonded N), depicted in Fig. 3. The base donates charge through the orbital dominated by the nitrogen lone pair to the σ antibonding orbital of the acid located in the region of the hydroxyl hydrogen atom, and the overlap of these two orbitals is maximized when the OH…N alignment is linear.

3.2. Blue-shifting Hydrogen-bonded Complexes

The blue-shifting hydrogen bond was recognized as an important variant of the conventional hydrogen bond by Hobza and Havlas, who reviewed the properties of a number of examples of complexes demonstrating this phenomenon in 2000.[22] The bases, B, taking part in a blue-shifting hydrogen bond interaction are essentially drawn from the same range of electron donors as those found in orthodox hydrogen bonds. The proton donors, however, are usually those in which the AH bond is fairly non-polar. Most examples of this new type of interaction involve CH, PH or SH groups. Otherwise the same classification into donor and acceptor of either proton or electron holds as described above. The major distinction between the two families of interaction is in their physical manifestations; blue-shifting hydrogen bonds are characterized by a *decrease* of the AH bond length, a shift of the AH stretching wavenumber to the *blue* and a *reduction* of the AH stretching band intensity. We present as examples of blue-shifting hydrogen bonds the homodimers of formaldehyde,[23] phosphine[24] and methane,[10] and the heterodimers $CH_4.H_2O$, $H_2S.CH_4$[25] and $HCN.F_2$.[4] The optimized structures of the homodimers are shown in Fig. 4 and those of the heterodimers in Fig. 5.

Table 4 Interaction energies of some blue-shifting hydrogen-bonded complexes.

Homodimers		Heterodimers	
Complex	ΔE/kJ mol^{-1}	Complex	ΔE/kJ mol^{-1}
$(H_2CO)_2$	–49.9	$CH_4.H_2O$	–4.3
$(PH_3)_2$	–2.2	$H_2S.CH_4$	–4.0
$(CH_4)_2$	–0.6	$HCN.F_2$	–0.8

The interaction energies of these six aggregates are presented in Table 4. Apart from the example of $(H_2CO)_2$, the complexes are all extremely weakly bound. This observation reflects the minimal degree of bond polarity found in the CH, PH and SH proton donor groups, resulting in conditions unfavourable for strong interaction.

The structural and spectroscopic properties of this group of complexes are shown in Tables 5 and 6. The bonded CH and PH bonds of the H_2CO and PH_3 homodimers undergo small decreases of bond length, while in the case of $(CH_4)_2$ one of the two bonded CH bond lengths increases and the other decreases, but by less than 0.01 pm, close to the limit of precision of the calculations, consistent with the extremely small interaction energy. The wavenumbers of the partly decoupled CH stretching modes of $(H_2CO)_2$ both increase, by a magnitude comparable with the decreases in the $CH_3OH.CH_3F$ and $CH_3OH.CH_3Cl$ complexes, although the $(H_2CO)_2$ interaction energy is five times greater than those in the methanol-halogen base complexes. The wavenumber shifts of the PH stretching modes of the four equivalent bonded PH groups in $(PH_3)_2$ are small, but consistently to the blue. In $(CH_4)_2$, however, only one of the CH

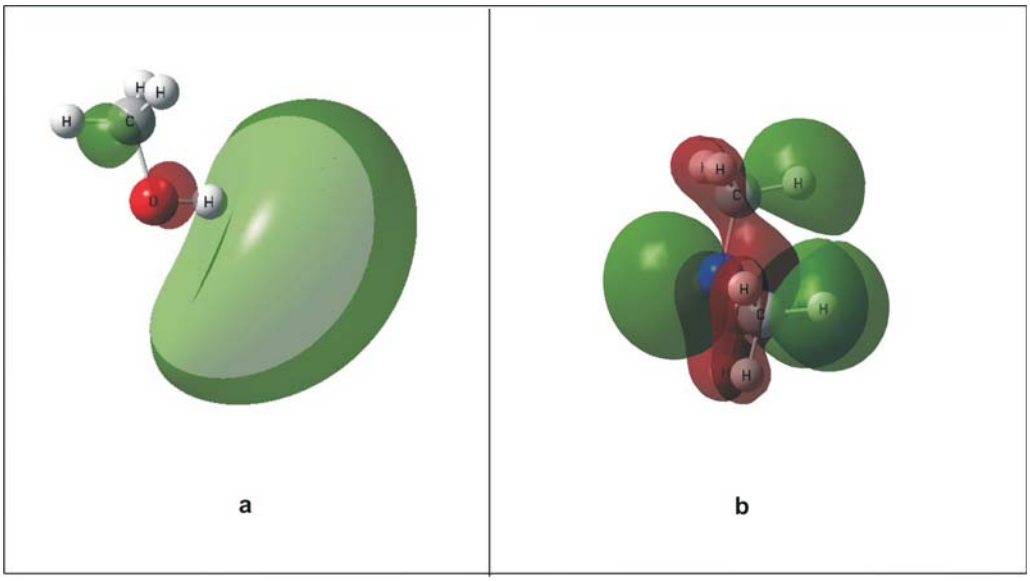

Figure 3 Plots of (**a**) the 8a′ (LUMO) (OH σ^*) orbital of CH_3OH and (**b**) the $6a_1$ (HOMO) (non-bonding N) orbital of $(CH_3)_3N$.

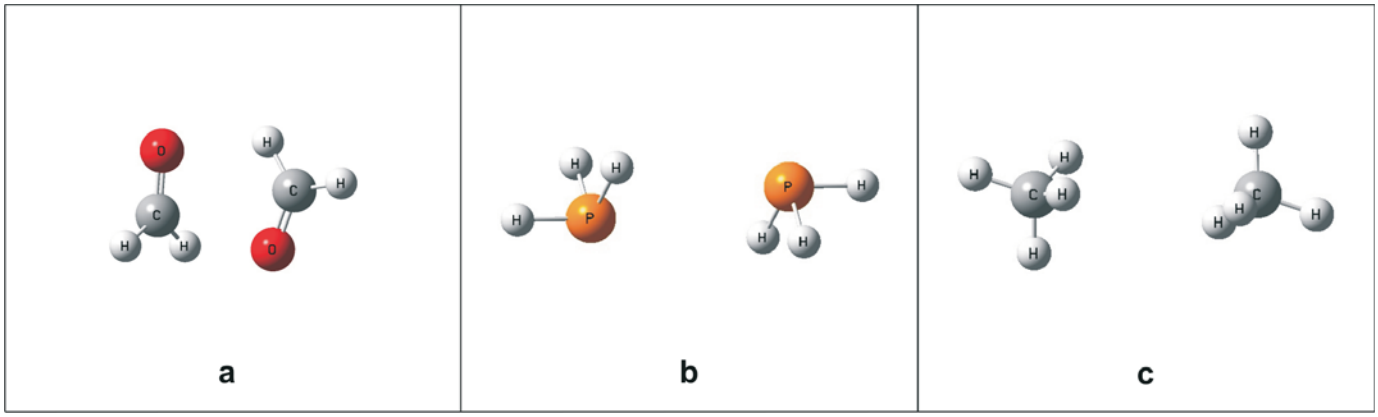

Figure 4 The optimized structures of the dimers of (**a**) H_2CO, (**b**) PH_3 and (**c**) CH_4.

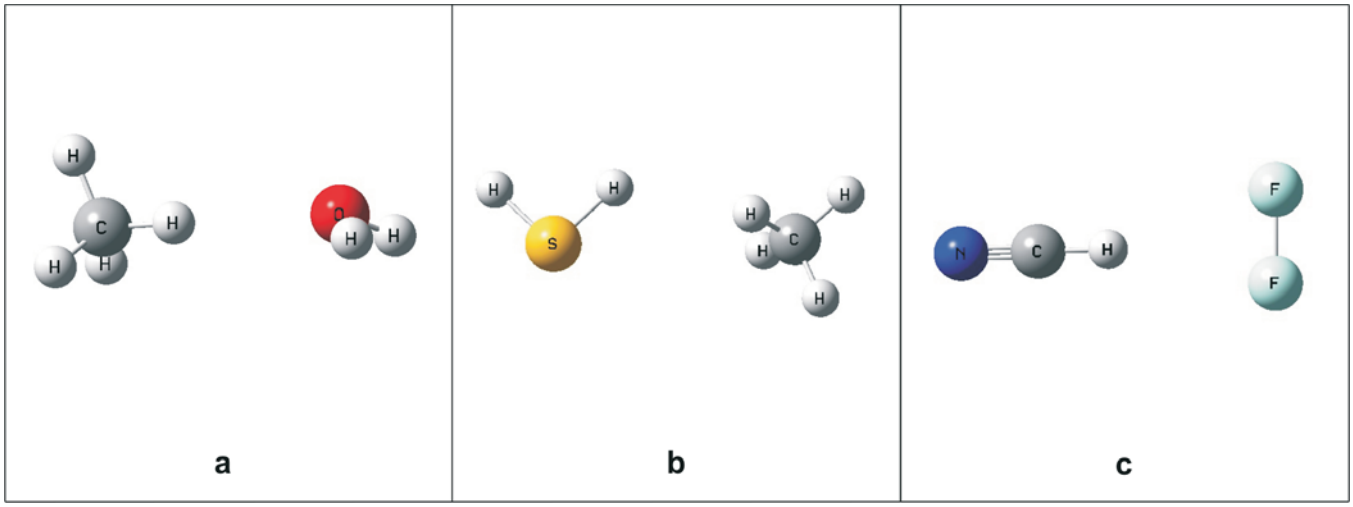

Figure 5 The optimized structures of the (**a**) $CH_4.H_2O$, (**b**) $H_2S.CH_4$ and (**c**) $HCN.F_2$ complexes.

stretching shifts is positive, while the other three are negative. These shifts are minimal, however, confirming that the methane dimer is probably barely bound at all. The corresponding changes for the heterodimers follow the same trend, but in the case of $H_2S.CH_4$ one is to the red and the other is to the blue, although the shifts are both less than 1 cm^{-1}. This complex provides another example of an extremely weak adduct, in which the structural and spectroscopic perturbations are close to

Table 5 Structural and spectroscopic properties of some blue-shifting hydrogen-bonded homodimers.

Complex	r(AH)(bonded)/pm	Δr(AH)(bonded)/pm	Mode	$\bar{\nu}$(AH)/cm^{-1}	Δ$\bar{\nu}$(AH)/cm^{-1}
$(H_2CO)_2$	110.31	–0.17	$\nu_a(CH_2)$	3075.8	28.8
			$\nu_s(CH_2)$	2992.1	16.6
$(PH_3)_2$	140.84	-0.07	$\nu_a(PH_2)$	2528.4	6.9
			$\nu_a(PH_2)$	2524.8	3.2
			$\nu_s(PH_2)$	2522.6	1.1
			$\nu_s(PH_2)$	2522.0	0.5
$(CH_4)_2$	109.019	–0.006	$\nu_a(CH_2)$	3212.2	1.4
	109.031	0.006	$\nu_a(CH_2)$	3210.5	–0.3
			$\nu_s(CH_2)$	3072.6	–1.0
			$\nu_s(CH_2)$	3072.6	–1.0

Table 6 Structural and spectroscopic properties of some blue-shifting hydrogen-bonded heterodimers.

Complex	r(AH)(bonded)/pm	Δr(AH)(bonded)/pm	Mode	$\bar{\nu}$(AH)/cm^{-1}	Δ$\bar{\nu}$(AH)/cm^{-1}
$CH_4.H_2O$	108.99	–0.04	ν(CH)	3218.9	8.0
$H_2S.CH_4$	133.33	–0.02	$\nu_a(SH_2)$	2837.0	0.9
			$\nu_s(SH_2)$	2816.3	–0.7
$HCN.F_2$	106.78	–0.02	ν(CH)	3488.6	5.7

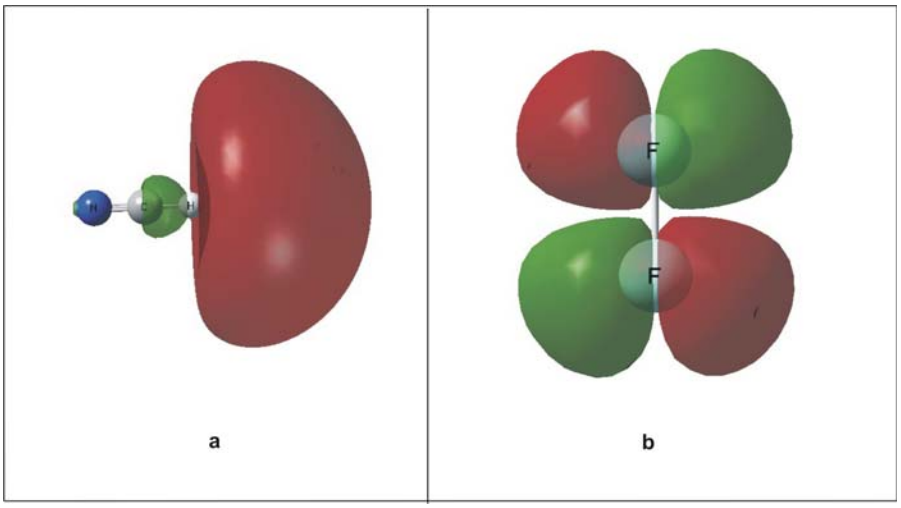

Figure 6 Plots of (**a**) the 6σ (LUMO) (CH σ*) orbital of HCN and (**b**) the 1π_g (HOMO) (FF π*) orbital of F_2.

the limit of detection by the computational method.

The molecular orbital interactions, and their influence on the structures, may be illustrated by reference to the LUMO (6σ) of HCN (CH σ antibonding) and the HOMO (1π_g) of F_2 (FF π antibonding), shown in Fig. 6. The HOMO of F_2 donates charge to the LUMO of HCN. Maximum overlap alignment of these two orbitals, with the correct phase relationships, leads to an L-shaped structure. The contrasting properties of blue-shifting hydrogen bonds relative to their conventional analogues have been interpreted in terms of electron charge redistribution as follows.[22,26] Contrasting HOH…OH_2 (red-shifted) with F_3CH…OH_2 (blue-shifted), in the first case charge is donated from an oxygen lone pair orbital of the electron donor to the OH σ antibonding orbital of the proton donor, while in the second case the main transfer is to the CF σ antibonding orbital of CHF_3, remote from the primary site of interaction, with little build-up of charge in the CH σ antibonding orbital. This may imply that candidates as proton donors in blue-shifting hydrogen-bonded complexes require a nearby site of high electron density, such as a fluorine atom, in order to facilitate this electron redistribution.

3.3. Halogen-bonded Complexes

The concept of the halogen bond was first proposed by Legon, in explaining the results of his Fourier transform microwave experiments on the gas-phase complex formed between water and molecular chlorine.[27] The complex was observed to have an O…Cl-Cl bonded structure, with an almost linear arrangement of the heavy atoms. Legon described the interaction as a 'chlorine bond', and several examples of similar interactions involving other halogens and interhalogens have since been reported, represented by XY…B, where X, Y = F, Cl, Br or I and B = N, O, P or S. The nature of the interaction was attributed to a donation of charge from the axial non-bonding orbital located on the oxygen atom to the ClCl σ antibonding orbital. The analogy with a hydrogen bond is clear; replacing the electron acceptor Cl_2 by a second H_2O molecule, the hydrogen bond in the resulting water dimer is formed by donation from an oxygen lone pair of one molecule into the OH σ antibonding orbital of the other. It would be interesting to explore what other similarities exist between the halogen bond and the hydrogen bond.

Table 7 Interaction energies of some halogen-bonded complexes.

H_2O complexes		NH_3 complexes	
Complex	ΔE/kJ mol^{-1}	Complex	ΔE/kJ mol^{-1}
$H_2O.F_2$	+1.2	$NH_3.F_2$	–1.7
$H_2O.Cl_2$	–4.5	$NH_3.Cl_2$	–11.5
$H_2O.Br_2$	–8.4	$NH_3.Br_2$	–19.3

We have investigated the six complexes formed between water and ammonia, as electron donors, and molecular fluorine, chlorine and bromine as electron acceptors. Examples of the resulting structures, of $H_2O.Cl_2$ and $NH_3.Br_2$, are shown in Fig. 7. The interaction energies of the six complexes are presented in Table 7. The interactions are typically weak, and indeed that between H_2O and F_2 indicates an unstable complex relative to the separated monomers. The strengths of interaction correlate fairly well with the polarizabilities of the halogens with, as we

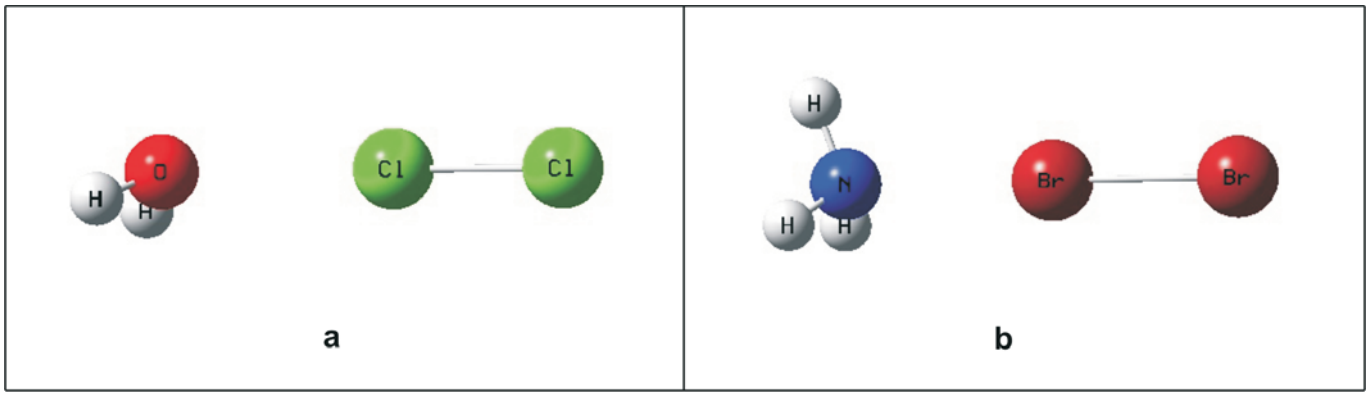

Figure 7 The optimized structures of the (**a**) $H_2O.Cl_2$ and (**b**) $NH_3.Br_2$ complexes.

Table 8 Structural properties of some halogen-bonded complexes.

Complex	r(AH)/pm	Δr(AH)/pm	r(XX)/pm	Δr(XX)/pm	∠HAH/deg	Δ∠HAH/deg
$H_2O.F_2$	96.02	0.07	142.39	0.72	103.471	0.004
$H_2O.Cl_2$	96.04	0.09	203.38	0.93	103.72	0.26
$H_2O.Br_2$	96.06	0.11	231.76	1.07	103.91	0.45
$NH_3.F_2$	101.46	0.12	143.67	2.00	106.82	–0.47
$NH_3.Cl_2$	101.48	0.13	206.01	3.56	107.24	–0.06
$NH_3.Br_2$	101.51	0.17	235.18	4.48	107.46	0.17

Table 9 Spectroscopic properties of some halogen-bonded complexes.

Complex	$\Delta\bar{\nu}_1$/cm^{-1}	$\Delta\bar{\nu}_2$/cm^{-1}	$\Delta\bar{\nu}_3$/cm^{-1}	$\Delta\bar{\nu}_4$/cm^{-1}	$\Delta\bar{\nu}$(XX)/cm^{-1}
$H_2O.F_2$	–7.2	8.9	–8.0		–24.9
$H_2O.Cl_2$	–9.4	4.1	–10.4		–13.8
$H_2O.Br_2$	–12.7	5.6	–13.6		–7.6
$NH_3.F_2$	–9.1	12.8	–12.9	–17.0	–87.2
$NH_3.Cl_2$	–10.5	36.8	–13.4	–31.3	–65.4
$NH_3.Br_2$	–14.0	55.9	–16.9	–29.7	–39.4

have observed above, separate relationships for the two series (see Fig. 8).

The structural parameters of the complexes (the OH, NH and XX bond lengths and their increases on complexation, and the HOH and HNH angles and their changes) are shown in Table 8. There are minor changes in the OH and NH bond lengths, showing slight increases with increasing strength of interaction. The changes in the XX bond lengths are in the same direction, but are much more pronounced. The HOH and HNH angles open out slightly more with increased binding energy although, curiously, in the ammonia complexes, the angles are smaller than in the ammonia monomer for the F_2 and Cl_2 cases, and only for the $NH_3.Br_2$ complex does the value of the HNH angle exceed that of the uncomplexed monomer.

The wavenumber shifts of the intramolecular modes of the electron donors and of the XX stretching modes of the halogen sub-molecules are shown in Table 9. Here, ν_1 and ν_3 are the symmetric and antisymmetric H_2O or NH_3 stretching modes, ν_2 is the HOH bending mode of H_2O and the symmetric HNH bending mode of NH_3, and ν_4 is the corresponding antisymmetric bending vibration of NH_3. The stretching modes are shifted to the red, and these shifts increase monotonically with increasing strength of interaction. The ν_2 modes are shifted to the blue (a typical observation for hydrogen-bonded complexes[20]), but the shift for the $H_2O.F_2$ complex appears to be exaggerated. This anomaly is connected with the fact that this complex is dissociative. The ν_4 modes, on the other hand, are red-shifted, but the changes are not monotonic. The stretching modes of the electron acceptors are all shifted to lower wavenumber, but the shifts are inversely proportional to the interaction energies. This is due to the fact that complex formation populates the XX σ antibonding orbitals, thereby reducing the stretching force constants and decreasing the stretching wavenumbers. However, due to electronic redistribution, increase in the charge densities in the antibonding orbitals also leads to an increase in the population of the corresponding σ bonding orbitals, and for the stronger complexes these two effects partly cancel one another, so that the XX stretching wavenumbers now approach more closely their values in the halogen monomers.

Figure 9 depicts the LUMO ($3\sigma_u$*) of F_2 (σ antibonding) and the HOMO ($1b_1$) of H_2O (out-of-plane oxygen non-bonding) in the $H_2O.F_2$ complex. Maximum overlap of these frontier orbitals,

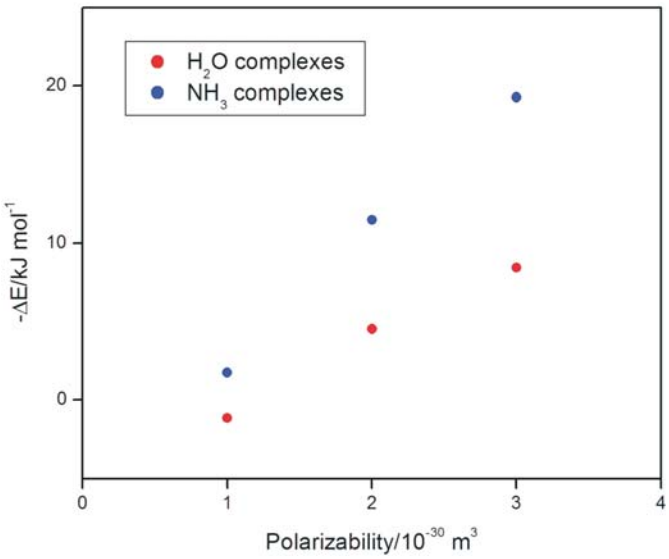

Figure 8 Plots of the interaction energies of the complexes of H_2O and NH_3 with F_2, Cl_2 and Br_2 *versus* the polarizabilities of the halogens.

with donation from H_2O to F_2, would yield a complex structure with the F-F…O axis perpendicular to the water plane. Interaction with the HOMO-1 orbital of H_2O ($3a_1$ – axial oxygen non-bonding), on the other hand, as shown in Fig. 10, would result in a planar complex. The fact that the optimized structure of the complex indicates a slightly non-planar structure (see Fig. 7 for the structure of the comparable $H_2O.Cl_2$ complex) demonstrates that the water orbital responsible for electron donation is in fact a localized orbital formed from a linear combination of the $3a_1$ and $1b_1$ non-bonding orbitals. As a consequence of the lowering of the symmetry of the water fragment from C_{2v} to C_s on complexation, the $3a_1$ and $1b_1$ orbitals are allowed to mix, resulting in a hybrid orbital containing predominantly $3a_1$ character, with only a small contribution from $1b_1$.

3.4. Electron Donor-acceptor Complexes

Many of our recent publications[5–8] have reported the properties of a range of complexes containing boron trifluoride as an electron acceptor (Lewis acid or electrophile). These complexes have been known for many years; a fifty-year old review by Greenwood and Martin listed over 300 such complexes which had been investigated at that time.[28] The common feature of these aggregates is the presence of a sterically accessible BF π antibonding orbital (the LUMO – $2a_2''$) projecting normal to the BF_3 plane, as illustrated in Fig. 11, which may receive charge donation from a lone pair orbital of a partner electron donor (Lewis base or nucleophile). We have studied the complexes of BF_3 with the series of nitrogen donors NH_3,[29] CH_3NH_2, $(CH_3)_2NH$ and $(CH_3)_3N$ in order to explore the effect of successive methylation on the properties of the complexes. We have also included the parallel set of complexes with the oxygen and

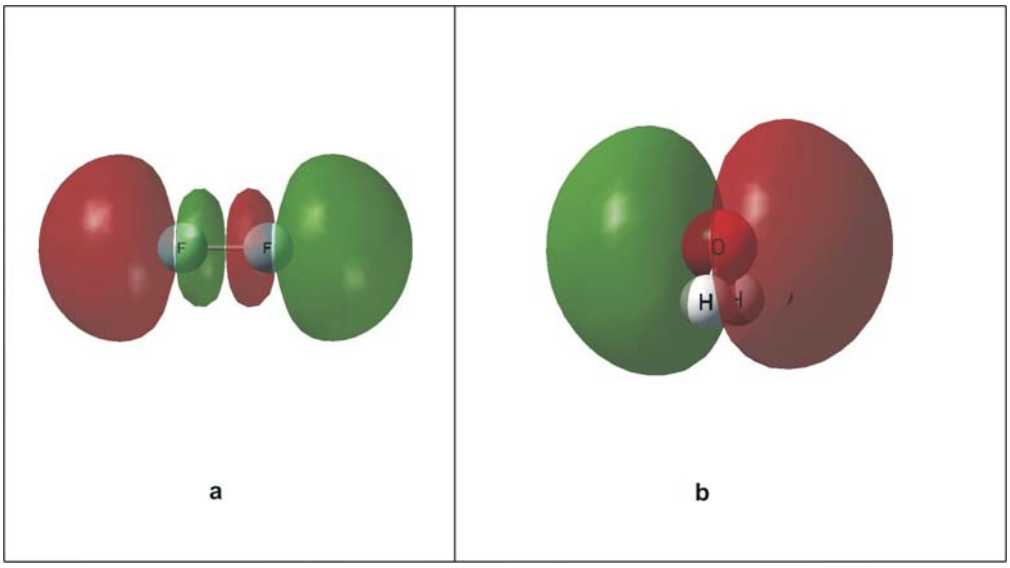

Figure 9 Plots of (**a**) the $3\sigma_u$* (LUMO) (FF σ*) orbital of F_2 and (**b**) the $1b_1$ (HOMO) (non-bonding O) orbital of H_2O.

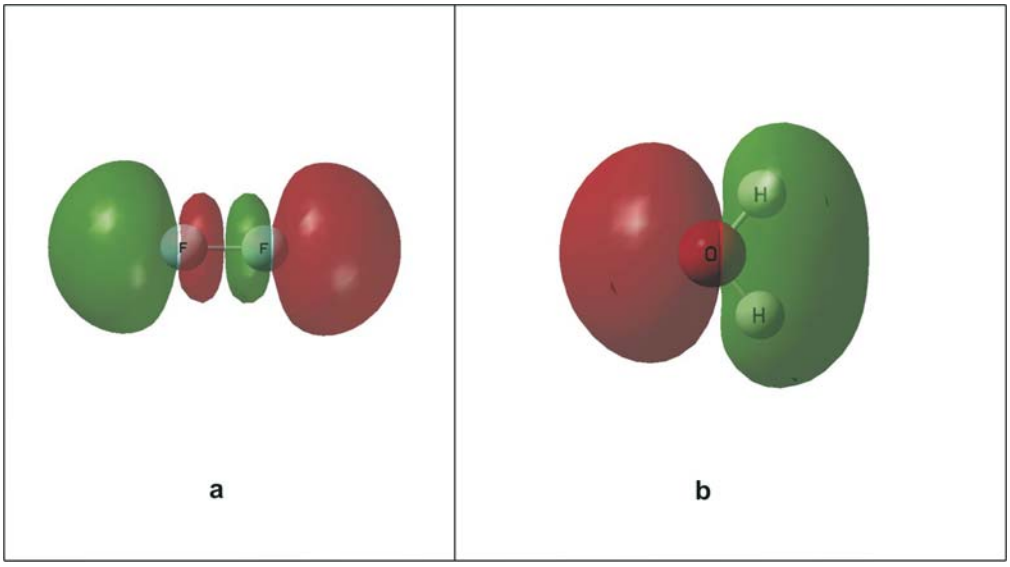

Figure 10 Plots of (**a**) the $3\sigma_u$* (LUMO) (FF σ*) orbital of F_2 and (**b**) the $3a_1$ (HOMO-1) (non-bonding O) orbital of H_2O.

sulphur donors H_2O and H_2S,[30] CH_3OH and CH_3SH,[31] and $(CH_3)_2O$ and $(CH_3)_2S$.[32] Moreover, in order to examine the relative propensities of nitrogen, oxygen, sulphur and halogen bases to form EDA complexes with BF_3, we have also studied the complexes $BF_3.F_2$, $BF_3.Cl_2$, $BF_3.ClF$ and $BF_3.FCl$.[8] The optimized structures of a sample of these EDA adducts are shown in Fig. 12.

The interaction energies are collected in Table 10. Within each series the interaction energies increase monotonically with the

Table 10 Interaction energies of some electron donor-acceptor complexes of boron trifluoride.

Complex	ΔE/kJ mol^{-1}	Complex	ΔE/kJ mol^{-1}
$BF_3.NH_3$	–160.34	$BF_3.H_2S$	–6.9
$BF_3.CH_3NH_2$	–191.7	$BF_3.CH_3SH$	–55.5
$BF_3.(CH_3)_2NH$	–209.7	$BF_3.(CH_3)_2S$	–93.6
$BF_3.(CH_3)_3N$	–217.2	$BF_3.F_2$	–0.4
$BF_3.H_2O$	–56.7	$BF_3.FCl$	–3.5
$BF_3.CH_3OH$	–98.0	$BF_3.ClF$	+1.5
$BF_3.(CH_3)_2O$	–116.6	$BF_3.Cl_2$	+1.2

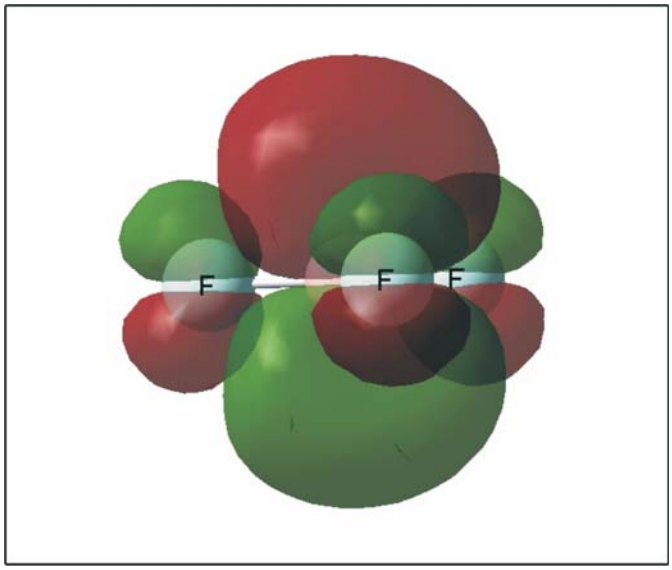

Figure 11 Plot of the $2a_2''$ (LUMO) (BF π*) orbital of BF_3.

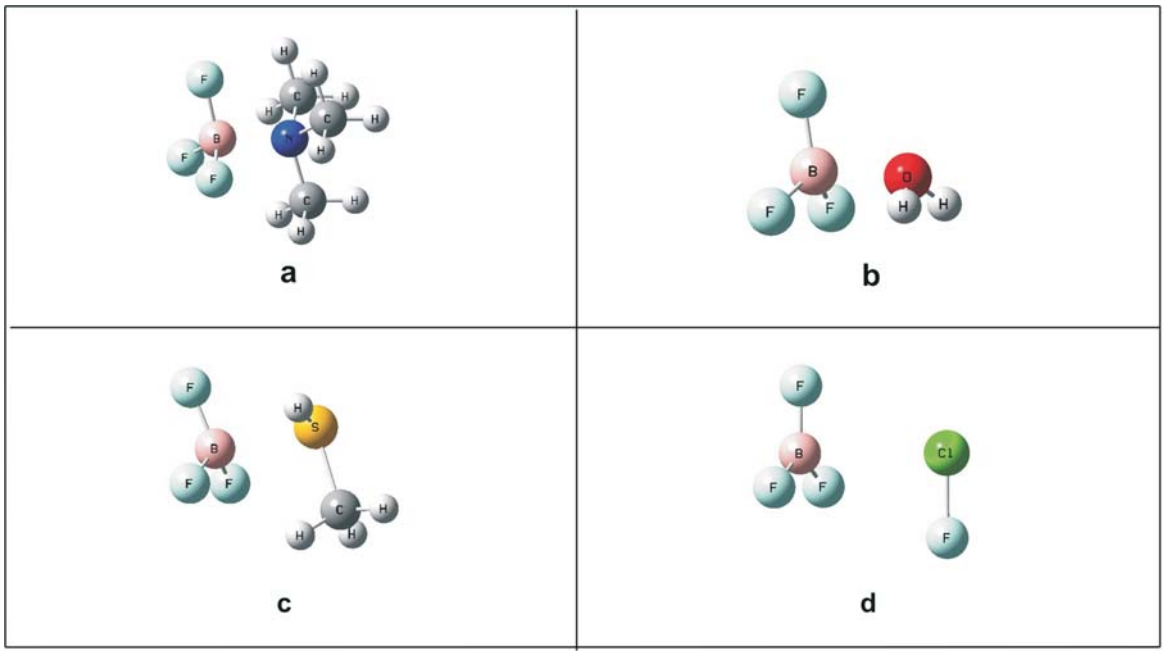

Figure 12 The optimized structures of the (**a**) $BF_3.(CH_3)_3N$, (**b**) $BF_3.H_2O$, (**c**) $BF_3.CH_3SH$ and (**d**) $BF_3.ClF$ complexes.

number of substituted methyl groups, and for the same number of methyl groups the strength of binding increases in the order S < O < N. There is a very large difference in the typical orders of magnitude of the interaction energies of the halogen base complexes compared with those with N, O or S bases. In fact, as we found for the HCN.F_2 complex, the interaction energies of BF_3.ClF and $BF_3.Cl_2$ turned out to be positive, indicating that these complexes are unstable relative to the separate monomers. The interaction energies of the N, O and S base complexes are plotted against the gas phase basicities of the bases in Fig. 13. Here, the first row bases follow the same trend line and the second row bases a separate relationship.

Table 11 reports the intermolecular structural parameters of the N, O and S bases. The B…X separations (X = N, O and S) decrease steadily with increasing basicity, although the spread of distances for the nitrogen bases is rather small. The first member of each series (NH_3, H_2O and H_2S) displays a B…X separation noticeably larger than for the methylated analogues, indicating that binding energy increases steeply on substitution of the first methyl group and is less affected by subsequent substitution. The mean FB…X angles, which are a measure of the extent of distortion of the BF_3 fragment from planarity, are also directly proportional to the binding energy. The corresponding structural parameters for the halogen base complexes are presented in Table 12. The complexes bound through a fluorine atom have significantly smaller B…X separations compared with the chlorine-bound analogues, reflecting the fact that the F-bound complexes are genuinely bound, while the Cl-bound complexes are dissociative. Likewise the mean B…XY angles of $BF_3.F_2$ and BF_3.FCl are noticeably larger (close to the tetrahedral angle) than those of the complexes with ClF and Cl_2 (almost perpendicular). This indicates that the orbitals of the base involved in the formation of the complex in the two fluorine

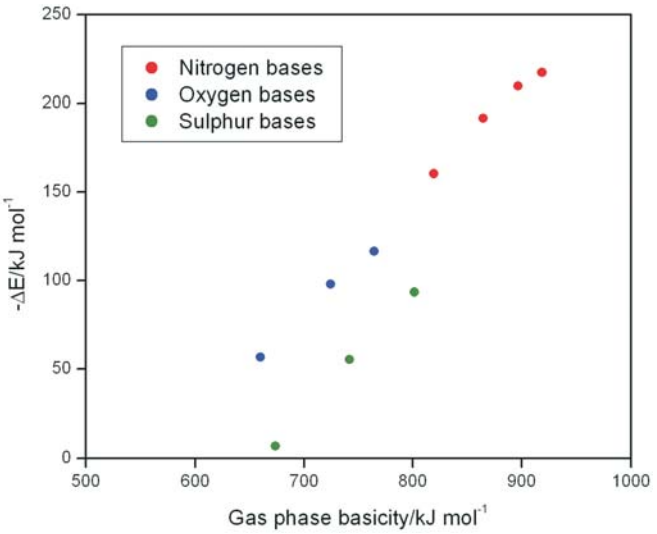

Figure 13 Plots of the interaction energies of some complexes of BF_3 *versus* the gas phase basicities of the electron donors.

Table 11 Intermolecular structural parameters of some electron donor-acceptor complexes of boron trifluoride (nitrogen, oxygen and sulphur bases).

Complex	R(B…X)/pm	Mean ∠FB…X /deg
$BF_3.NH_3$	166.87	104.17
$BF_3.CH_3NH_2$	165.25	104.65
$BF_3.(CH_3)_2NH$	165.19	105.06
$BF_3.(CH_3)_3N$	165.86	105.41
$BF_3.H_2O$	181.64	100.13
$BF_3.CH_3OH$	169.79	102.05
$BF_3.(CH_3)_2O$	167.93	102.86
$BF_3.H_2S$	290.87	92.90
$BF_3.CH_3SH$	223.08	100.86
$BF_3.(CH_3)_2S$	212.55	102.64

Table 12 Intermolecular structural parameters of some electron donor-acceptor complexes of boron trifluoride (fluorine and chlorine bases).

Complex	R(B…X)/pm	Mean ∠B…XY /deg
$BF_3.F_2$	275.11	101.76
BF_3.FCl	252.33	114.52
BF_3.ClF	316.74	90.18
$BF_3.Cl_2$	304.83	95.03

Table 13 Mean BF_3 ν_3 wavenumber shifts of some electron donor-acceptor complexes of boron trifluoride (nitrogen, oxygen and sulphur bases).

Complex	$\Delta\bar{\nu}_3$/cm^{-1}	Complex	$\Delta\bar{\nu}_3$/cm^{-1}	Complex	$\Delta\bar{\nu}_3$/cm^{-1}
$BF_3.NH_3$	–210.9	$BF_3.H_2O$	–125.7	$BF_3.H_2S$	–21.8
$BF_3.CH_3NH_2$	–222.6	$BF_3.CH_3OH$	–174.3	$BF_3.CH_3SH$	–158.8
$BF_3.(CH_3)_2NH$	–243.6	$BF_3.(CH_3)_2O$	–188.8	$BF_3.(CH_3)_2S$	–204.2
$BF_3.(CH_3)_3N$	–249.1				

cases have some non-bonding sp^3 character, while in the case of the chlorine-bound species the Cl_2 and ClF orbitals are essentially atomic chlorine *3p* orbitals, consistent with the coordination angles typical of first row and second row electron donors.

The spectroscopic properties of the complexes with the N, O and S bases are exemplified by the mean shifts of the antisymmetric BF_3 stretching mode, ν_3, shown in Table 13. All the shifts are to the red, and within each series they become more negative monotonically with increasing methyl substitution, as we found for the interaction energies and the intermolecular structural parameters. Also, for the same number of methyl groups, the shifts are usually in the order N > O > S. The ν_3 wavenumber shifts of the BF_3 fragments in EDA complexes have been observed to be good indicators of the strength of binding in these complexes,[33] and the results presented here are found to be consistent with this generalization.

4. Conclusions

The common features of all the interactions described above are characterized by donation of electronic charge, either from a lone pair orbital associated with, e.g., a nitrogen or oxygen atom, or a F_2 π^* orbital (as in the case of $HCN.F_2$) of one molecule, to either a σ^* orbital (e.g. OH, CH, SH, ClCl, etc.) or a π^* orbital (as in the BF_3 complexes) of the other. Whether a particular interaction should be classified as a hydrogen-bonded, in either of its varieties, a halogen-bonded or a donor-acceptor association, will be determined by the natures of the particular combination of interacting monomers involved. Thus, application of the principles described above to the prediction of the properties of a molecular complex formed between any pair of interacting monomer species should result in a reasonably accurate picture of the nature of the adduct, which may then be used as a guide in the interpretation of the molecular structures and spectra of the complex. A full global rationalization of all the various forms of molecular interaction in terms of common bonding characteristics, however, must await further exploration of a greater variety of associated species.

Acknowledgements

This material is based upon work supported by the National Research Foundation under Grant Number 2053648. Any opinion, findings and conclusions or recommendations expressed in this material are those of the author and do not necessarily reflect the views of the National Research Foundation. The author also acknowledges the financial assistance of the University of KwaZulu-Natal Research Fund, through its support of the Centre for Theoretical and Computational Chemistry, and the valuable contributions of Julie Altmann, Bradley Bricknell, Leslie Glasser, Magan Govender, Gert Kruger, Laurelly Millar, Lawrence Nxumalo, Kishore Singh and Geoff Yeo.

References

1 G.A. Yeo and T.A. Ford, *Can. J. Chem.,* 1991, **69**, 632–637.
2 G.A. Yeo and T.A. Ford, *Struct. Chem.,* 1992, **3**, 75–93.
3 B.C. Bricknell, T.M. Letcher and T.A. Ford, *S. Afr. J. Chem.,* 1995, **48**, 142–153.
4 L.J. Millar and T.A. Ford, *J. Mol. Structure,* 2005, **744–747**, 195–205.
5 L.M. Nxumalo, M. Andrzejak and T.A. Ford, *J. Chem. Inf. Comput. Sci.*, 1996, **36**, 377–384.
6 T.A. Ford and D. Steele, *J. Phys. Chem.,* 1996, **100**, 19336–19343.
7 S.A. Peebles, L. Sun, R.L. Kuczkowski, L.M. Nxumalo and T.A. Ford, *J. Mol. Structure,* 1998, **471**, 235–242.
8. G.A. Yeo and T.A. Ford, *J. Mol. Structure (Theochem),* 2006, **771**, 157–164.
9 T.A. Ford, S.F. Agnew and B.I. Swanson, *J. Mol. Structure,* 1993, **297**, 265–275.
10 M.G. Govender and T.A. Ford, *J. Mol. Structure,* 1999, **480–481**, 219–229.
11 M. Venayagamoorthy and T.A. Ford, *J. Mol. Structure,* 2003, **651–653**, 223–229.
12 L.M. Nxumalo, E.K. Ngidi and T.A. Ford, *J. Mol. Structure,* 2006, **786**, 168–174.
13 Gaussian-98, Rev. A.7, M.J. Frisch, G.W. Trucks, H.B. Schlegel, G.E. Scuseria, M.A. Robb, J.R. Cheeseman, V.G. Zakrzewski, J.A. Montgomery, Jr., R.E. Stratmann, J.C. Burant, S. Dapprich, J.M. Millam, A.D. Daniels, K.N. Kudin, M.C. Strain, O. Farkas, J. Tomasi, V. Barone, M. Cossi, R. Cammi, B. Mennucci, C. Pomelli, C. Adamo, S. Clifford, J. Ochterski, G.A. Petersson, P.Y. Ayala, Q. Cui, K. Morokuma, D.K. Malick, A.D. Rabuck, K. Raghavachari, J.B. Foresman, J. Cioslowski, J.V. Ortiz , A.G. Baboul, B.B. Stefanov, G. Liu, A. Liashenko, P. Piskorz, I. Komaromi, R. Gomperts, R.L. Martin, D.J. Fox, T. Keith, M.A. Al-Laham, C.Y. Peng, A. Nanayakkara, C. Gonzalez, M. Challacombe, P.M.W. Gill, B. Johnson, W. Chen, M.W. Wong, J.L. Andres, M. Head-Gordon, E.S. Replogle and J.A. Pople, Gaussian, Inc., Pittsburgh, PA, 1998.
14 C. Møller and M.S. Plesset, *Phys. Rev.,* 1934, **46**, 618–622.
15 R. Krishnan, J.S. Binkley, R. Seeger and J.A. Pople, *J. Chem. Phys.,* 1980, **72**, 650–654.
16 T. Clark, J. Chandrasekhar, G.W. Spitznagel and P. von R. Schleyer, *J. Comput. Chem.,* 1983, **4**, 294–301.
17 B. Liu and A.D. McLean, *J. Chem. Phys.,* 1973, **59**, 4557–4558.
18 S.F. Boys and F. Bernardi, *Mol. Phys.,* 1970, **19**, 553–556.
19 W.M. Latimer and W.H. Rodebush, *J. Am. Chem. Soc.,* 1920, **42**, 1419–1433.
20 G.C. Pimentel and A.L. McClellan, *The Hydrogen Bond,* W.H. Freeman, San Francisco, 1960, pp. 70,71.
21 E.P.L. Hunter and S.G. Lias, *J. Phys. Chem. Ref. Data,* 1998, **27**, 413–656.
22 P. Hobza and Z. Havlas, *Chem. Rev.,* 2000, **100**, 4253–4264.
23 T.A. Ford and L. Glasser, *J. Mol. Structure (Theochem),* 1997, **398–399**, 381–394.
24 J.A. Altmann, M.G. Govender and T.A. Ford, *Mol. Phys.*, 2005, **103**, 949–961.
25 M.G. Govender and T.A. Ford, *J. Mol. Structure (Theochem),* 2003, **630**, 11–16.
26 X. Li, L.Liu and H.B. Schlegel, *J. Am. Chem. Soc.*, 2002, **124**, 9639–9647.
27 A.C. Legon, *Chem. – Eur. J.,* 1998, **4**, 1890–1897.
28 N.N. Greenwood and R.L. Martin, *Quart. Rev.,* 1954, **8**, 1–39.
29 L.M. Nxumalo, M. Andrzejak and T.A. Ford, *Vibr. Spectrosc.,* 1996, **12**, 221–235.
30 G.A. Yeo and T.A. Ford, *S. Afr. J. Chem.,* 2006, **59**, 129–134.
31 T.A. Ford, *J. Mol. Structure,* 2007, **834–836**, 30–41.
32 L.M. Nxumalo and T.A. Ford, *J. Mol. Structure (Theochem),* 1996, **369**, 115–126.
33 T.A. Ford, Molecular complexes: perturbations of vibrational spectra, in *Encyclopaedia of Computational Chemistry (online edition),* (P. von R. Schleyer, H.F. Schaefer III, P.R. Scheiner, W.L. Jorgensen, W. Thiel, R.C. Glen, eds.), John Wiley and Sons, Ltd., Chichester, U.K. Article online posting date: 15 June 2004. DOI: 10.1002/0470845015.cu0033.